Temperature-dependent Plasmons and Their Damping Rates for Graphene with a Finite Energy Bandgap

Andrii Iurov[1], Godfrey Gumbs[2,3], Danhong Huang[4], and V. Silkin[3]
[1] *Center for High Technology Materials, University of New Mexico, Albuquerque, NM 87106*
[2] *Department of Physics and Astronomy, Hunter College of the City University of New York, 695 Park Avenue, New York, NY 10065*
[3] *Donostia International Physics Center (DIPC), P de Manuel Lardizabal, 4, 20018, San Sebastian, Basque Country, Spain*
[4] *Air Force Research Laboratory, Space Vehicles Directorate, Kirtland Air Force Base, NM 87117*
(Dated: April 20, 2015)

We obtained numerical and closed-form analytic expressions for finite-temperature plasmon dispersion relations for intrinsic graphene in the presence of a finite energy gap in the energy spectrum. The calculations were carried out using the random-phase approximation. The analytic results have been derived in the high temperature regime and long-wavelength limit. We have found that the plasmon damping rate decreases in the presence of a band gap. Our method of calculation could also be applied to silicene and other buckled honeycomb lattice structures. The finite-temperature plasmon dispersion relations are presented when a single graphene layer is Coulomb coupled to a semi infinite conductor. Both cases of gapless and gapped monolayer graphene have been investigated when a thick substrate is in their proximity. Both the plasmon excitation frequency and damping rate are linear functions of the in-plane wave vector in the long wavelength limit when a monolayer interacts with a conducting substrate which is not the case for free-standing pristine or gapped graphene.

I. INTRODUCTION

Plasmons in grpahene represent one of the most interesting and actively studied fields, from both fundamentally theoretical[1–3,7–10] and experimental or technological points of view[4–6]. Graphene plasmons are especially important, partially because of their versatile frequency range which may be adjusted by varying the doping concentrations of its mobile carriers and energy band gap. Consequently, graphene has several potential device applications in optics, microscopy, nanolithography[26–28]. These studies in the area of plasmonics also extend to carbon-based structures such as fullerenes[11–16], carbon nanotubes[19,20], as well as the recently discovered silicon-based silicene and other buckled honeycomb lattice structures[17,18] with interesting roles played by the on-site potential differences between the sublattices. The main feature of the silicene energy dispersions is the energy gap, determined by the spin-orbit interaction. We believe that our theoretical formalism, here applied to gapped graphene, could also applicable in a straightforward way to silicene and germanene.

One of our goals is to investigate the way in which the energy band gap modifies the temperature-induced plasmon excitations and their damping rates in intrinsic (or undoped) graphene. Specifically, we distinguish the cases when the graphene layer is free-standing and when it is in close proximity with a thick conducting substrate. Clearly, such plasmon modes cannot be excited at $T = 0$ because of the absence of free carriers[10]. The gaplessness of graphene is an important factor in the thermal population of the valence and conduction bands with electrons and hole correspondingly. Since the finite temperature also results in the decay into particle-hole pairs, we are also interested to study how this decay (damping rate) depends on the temperature.

Closed-form analytic expressions for the long wavelength plasmon dispersion relation in gapped graphene as well as the dynamical polarization function were at $T = 0$ K initially reported by Pyatkovskiy in Ref.[8]. This important study demonstrated the existence of an extended range of wave vectors for the undapmed plasmons in the presence of a finite energy gap. This bandgap could be opened using a substrate or by exposing the graphene layer to circularly-polarized light.[21] The polarization function in this case was obtained analytically in Ref.[22].

We also consider finite-temperature plasmons in graphene which is Coulomb-coupled to a semi-infinite conducting substrate. For possible tailoring of the plasmon frequencies, graphene has been combined with prefabricated plasmonic nanoarrays and metamaterials in order to obtain hybrid plasmon devices[23–25]. Therefore, a thorough understanding of the dispersion and damping of plasmons in graphene interfacing with different kinds of substrates is necessary for producing innovative practical applications. We have investigated zero-temperature non-local plasmons in one of our previous studies[30], applying the theoretical formalism for a graphene layer interacting with a surface plasmon in a semi-infinite conductor was developed in[32,33]. The plasma instability in such systems was addressed in Ref.[29]. These results could be considered as a non-trivial extension of Ref.[31] in which a linear acoustic plasmon mode was obtained for two interacting graphene layers.

Some of our work is devoted to a careful calculation of the analytical results for the real and imaginary parts of the polarization function in the long wavelength limit and for the dispersion equation which yields the plasmon modes. The rest of the paper is organized as follows: in Sec.A we show that the finite-temperature polarization function used in Ref.[10] may be extended to the case of gapped graphene. After that, in Sec.II, we employ these results to gapped graphene to obtain the high-temperature plasmon dispersion relation in the long-wave limit, as well as the corresponding damping rate. This is an important contribution of our study. In Sec.III we derive the finite-temperature plasma dispersion relation for a graphene layer which is Coulomb-coupled to a semi-infinite substrate. These analytical results show novel non-trivial behavior, connected with the temperature dependence of each plasmon dispersion for both real and imaginary parts of the plasmon frequency. Finally, numerical results for the plasmon dispersion using the full polarization function for gapped graphene are presented in Sec.IV.

II. HIGH-TEMPERATURE PLASMON DISPERSION RELATION FOR GAPPED GRAPHENE

We now consider gapped graphene with energy dispersion: $\varepsilon(k) = \pm\sqrt{\Delta^2 + (\hbar v_F k)^2}$ where v_F is the fermi velocity and Δ is the energy gap between the valence (-) and conduction (+) bands and the polarization function in the long wavelength limit is given by

$$\Pi^0(q,\omega;\Delta) = \frac{2\mu}{\pi\hbar^2}\left(1 - \left(\frac{\Delta}{\mu}\right)^2\right)\frac{q^2}{\omega^2} \tag{1}$$

Equation (1) is only valid for $\Delta < \mu$. If $\Delta > \mu$, the valence band is completely empty and only inter-band transitions contribute to the plasmon excitations. The polarization functions is then given by

$$P_0(q,\omega;\Delta) = \frac{-2}{\pi\hbar}\frac{q^2}{v_F^2q^2-\omega^2}\left\{2\Delta + \frac{\hbar^2\left(v_F^2q^2-\omega^2\right) - 4\Delta^2}{\sqrt{v_F^2q^2-\omega^2}}\ \arcsin\left(\frac{v_F^2q^2-\omega^2}{v^2q^2-\omega^2-4\Delta^2/\hbar^2}\right)^{1/2}\right\}\ . \tag{2}$$

For $\Delta \to 0$, we have

$$P^0(q,\omega;\Delta\to 0) = \frac{-2g}{\pi\hbar}\frac{q^2}{v_F^2q^2-\omega^2}\left\{0 + \sqrt{v_F^2q^2-\omega^2}\arcsin 1\right\} = \frac{-ig}{4}\frac{q^2}{\sqrt{\omega^2-v_F^2q^2}} \tag{3}$$

which is similar to Eq. (B5).

We now turn our attention to evaluate the finite-temperature polarization

$$\Pi_T^{(0)}(q,\omega;\Delta) = \int_0^\infty d\,\mu'\frac{\Pi^0(q,\omega)}{4k_BT\left(\cosh\left[\frac{\mu-\mu'}{2kT}\right]\right)^2} = \tag{4}$$

$$= \int_0^{\mu'=\Delta} d\mu'\ \frac{P_0(q,\omega;\Delta)}{4k_BT\left(\cosh\left[\frac{\mu-\mu'}{2k_BT}\right]\right)^2} + \int_{\mu'=\Delta}^\infty d\,\mu'\ \frac{2\mu'}{\pi\hbar^2}\left(1-\left(\frac{\Delta}{\mu'}\right)^2\right)\frac{q^2/\omega^2}{4k_BT\left(\cosh\left[\frac{\mu-\mu'}{2k_BT}\right]\right)^2}$$

This expressions may be expressed as a sum of three parts, i.e., $\Pi_T^{(0)}(q,\omega;\Delta) = \sum_{j=1}^3 I_j$ with

$$I_1 = \int_0^{\mu'=\Delta}\frac{P_0(q,\omega;\Delta)}{4k_BT\left(\cosh\left[\frac{\mu-\mu'}{2k_BT}\right]\right)^2} = P_0(q,\omega;\Delta)\int_0^{\mu'=\Delta}\frac{1}{4k_BT\left(\cosh\left[\frac{\mu-\mu'}{2k_BT}\right]\right)^2} = \frac{1}{2}P_0(q,\omega;\Delta)\tanh\left[\frac{\Delta}{2k_BT}\right]$$

$$I_2 = \int_{\mu'=\Delta}^\infty d\,\mu'\frac{2\mu'}{\pi\hbar^2}\frac{q^2/\omega^2}{4k_BT\left(\cosh\left[\frac{\mu-\mu'}{2k_BT}\right]\right)^2} = \frac{2q^2}{\pi\hbar^2\omega^2}\left\{\frac{k_BT}{4}\ln 16 - \frac{\Delta}{2}\tanh\frac{\Delta}{2k_BT} + k_BT\ln\left[\cosh\frac{\Delta}{2k_BT}\right]\right\}$$

$$I_3 = \frac{\Delta^2q^2}{2k_BT\pi\hbar^2\omega^2}\int_\Delta^\infty\frac{d\,\mu'}{\mu'}\left(\cosh[(\mu-\mu')/(2k_BT)]\right)^{-2} \tag{5}$$

which are still to be evaluated.

A. Plasmon Dispersion relation (Re ω_p)

$$P_0(q,\omega;\Delta) = \frac{1}{2\pi\hbar^2}\frac{q^2}{v_F^2q^2-\omega^2}\left\{\frac{2\Delta}{\hbar}+\frac{\pi}{2}\sqrt{v_F^2q^2-\omega^2}\right\} \tag{6}$$

which consists of two terms, namely,

$$P_0(q,\omega;\Delta) = -\frac{i}{4\hbar}\frac{q^2}{\sqrt{\omega^2-v_F^2q^2}} - \frac{q^2}{\pi\hbar^2}\frac{\Delta}{\omega^2-v_F^2q^2}\ . \tag{7}$$

Therefore, for $T = 0$ K, the first correction which is associated with the energy gap is linear, real and negative. We now collect all the approximations from each term and write

$$I_1 = \frac{1}{2}P_0(q,\omega;\Delta)\tanh\left[\frac{\Delta}{2k_BT}\right] \backsimeq -\frac{1}{\pi\hbar^2}\frac{\Delta^2}{4k_BT}\frac{q^2}{\omega^2}\ . \tag{8}$$

We note that the zero-order term is purely imaginary. We present the next part as

$$I_2 = \frac{1}{\pi\hbar^2}\frac{k_BT}{2}\frac{q^2}{\omega^2}\ln 16 + \frac{2}{\pi\hbar^2}\frac{q^2}{\omega^2}G_1(T,\Delta)\,, \tag{9}$$

where

$$G_1(T,\Delta) = k_BT\ln\left[\cosh\frac{\Delta}{2k_BT}\right] - \frac{\Delta}{2}\tanh\frac{\Delta}{2k_BT} \backsimeq \frac{\Delta^2}{8k_BT} - \frac{\Delta^2}{4k_BT} = -\frac{\Delta^2}{8k_BT}\ . \tag{10}$$

In summary, we have

$$I_2 = \frac{2\ln 2}{\pi\hbar^2}k_BT\frac{q^2}{\omega^2} - \frac{1}{\pi\hbar^2}\frac{\Delta^2}{4k_BT}\frac{q^2}{\omega^2} \tag{11}$$

The remaining term is defined by

$$I_3 = \frac{1}{2\pi\hbar^2}\frac{\Delta^2}{2k_BT}\frac{q^2}{\omega^2}G_2(T,\Delta)\,, \tag{12}$$

where $G_2(T,\Delta)$ is a dimensionless integral defined as

$$G_2(T,\Delta) = \int_\Delta^\infty \frac{d\,\mu'}{\mu'}\frac{1}{\left(\cosh[(\mu-\mu')/(2k_BT)]\right)^2}\ . \tag{13}$$

The finite-temperature polarization function may be expressed as

$$\Pi_T^{(0)}(q,\omega;\Delta) = \frac{2\ln 2}{\pi\hbar^2}k_BT\frac{q^2}{\omega^2} - \frac{1}{\pi\hbar^2}\frac{\Delta^2}{4k_BT}\frac{q^2}{\omega^2}\left(1-G_2(T,\Delta)\right) \tag{14}$$

so that the dielectric function $\epsilon(q,\omega)$ is

$$\epsilon(q,\omega) = 1 - \frac{2\pi e^2}{\epsilon_s q}\Pi_T^{(0)}(q,\omega) = 1 - \frac{2\pi}{q}r_s\hbar v_F\Pi_T^{(0)}(q,\omega)\ . \tag{15}$$

From this, we deduce the temperature-induced plasma frequency of gapped graphene given by

$$\omega^2 = \frac{4}{\hbar}v_F\,r_S\,q\left[k_BT\ln 2 - \frac{\Delta^2}{4k_BT}\left(1-G_2(T,\Delta)\right)\right] \tag{16}$$

B. Evaluation of Integral G_2

Here, we are looking for an approximated result in analytic form for the following integral:

$$\int\limits_{\delta\ll 1}^{\infty} \frac{dx}{x\cosh^2 x} \ , \tag{17}$$

where $\delta = \Delta/k_BT$. In order to avoid the singularity appearing when $\delta \to 0$, we perform the integration by parts. Consequently, we obtain

$$\int\limits_{\delta}^{\infty} \frac{dx}{x\cosh^2 x} = \frac{\ln x}{\cosh^2 x}\bigg|_{\delta}^{\infty} + 2\int\limits_{\delta}^{\infty} dx\ \frac{\ln x \tanh x}{\cosh^2 x} \ . \tag{18}$$

We estimate each term when $\delta \to 0$ or $\Delta \ll k_BT$. We have

$$\frac{\ln x}{\cosh^2 x}\bigg|_{\delta}^{\infty} = -\ln\left(\frac{\Delta}{2k_BT}\right) \tag{19}$$

The second part is a small correction since the integrand does not diverge for $\delta \to 0$, using

$$\int\limits_{\delta}^{\infty} dx\ \frac{\ln x \tanh x}{\cosh^2 x} \backsimeq \int\limits_{0}^{\infty} dx\ \frac{\ln x \tanh x}{\cosh^2 x} = \frac{1}{6}\left(36\ln\mathcal{A}_{GK} - 7\ln 2 - 3(1+\gamma_{Eu})\right) \ , \tag{20}$$

where $\mathcal{A}_{GK} \backsimeq 1.2824$ is the Glaisher-Kinkelin constant, defined as

$$\mathcal{A} = \left\{\left(\prod_{s=1}^{\nu-1} s^s\right)\nu^{-\nu^2/2-\nu/2-1/12}\mathsf{e}^{\nu^2/4}\right\}_{\nu\to\infty} \tag{21}$$

and $\gamma_{Eu} = 0.5772$ is the Euler-Mascheroni constant, given by the following expression:

$$\gamma_{Eu} = \left\{\sum_{s=1}^{\nu}\frac{1}{s} - \ln\nu\right\}_{\nu\to 0} \tag{22}$$

Numerical integration gives

$$\int\limits_{0}^{\infty} dx\ \frac{\ln x \tanh x}{\cosh^2 x} = -0.1048 \tag{23}$$

and for $\delta = \Delta/(2k_BT) = 0.05$, we have

$$\int\limits_{\delta}^{\infty} dx\ \frac{\ln x \tanh x}{\cosh^2 x} = -0.1004 \ . \tag{24}$$

So, finally, we arrive at the result

$$G_2(T,\Delta) = \int\limits_{\delta\ll 1}^{\infty} \frac{dx}{x\cosh^2 x} \backsimeq -\ln\left(\frac{\Delta}{2k_BT}\right) \tag{25}$$

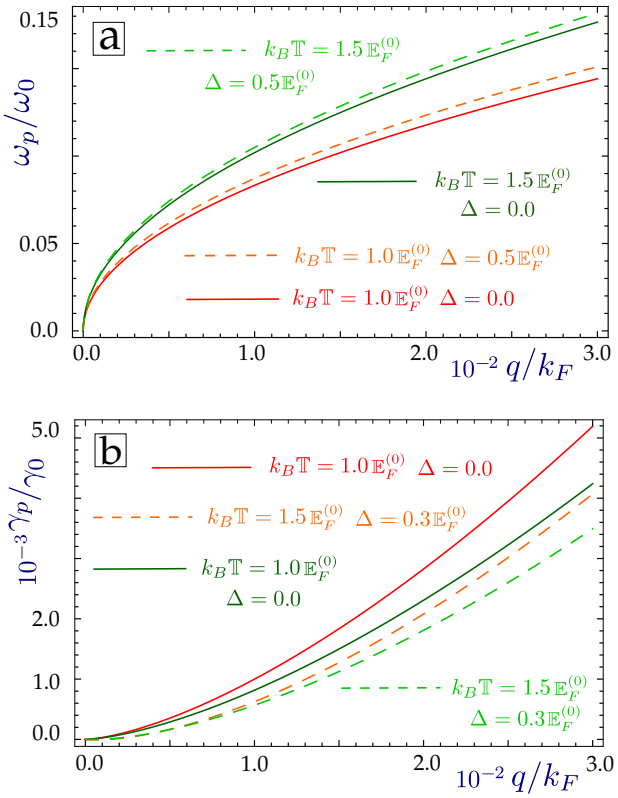

FIG. 1: (Color online) Plasmon frequency (a) in units of $\omega_0 = \left(4/\hbar v_F r_s k_F \mathbb{E}_F^{(0)} \log 2\right)^{1/2}$, where $\mathbb{E}_F^{(0)} = \hbar v_F k_F = 0.05\,eV$, and the damping rate ($b$) in units of $\gamma_0 = \left(\pi^2/64\ \hbar/\mathbb{E}_F^{(0)}\, r_s^3 v_F^3 k_F^3 \log 2\right)^{1/2}$ for high-temperature plasmons in gapped graphene. Plasmon dispersions are shown for $k_B\mathbb{T} = 1.0\,\mathbb{E}_F^{(0)}$ and $1.5\,\mathbb{E}_F^{(0)}$ and energy gap values $\Delta = 0.0$ and $0.5\mathbb{E}_F^{(0)}$, and damping rates for $\Delta = 0.0$ and $0.3\,\mathbb{E}_F^{(0)}$.

and the plasmon frequency in Eq. (16) is now given by the equation

$$\omega^2 = \frac{4}{\hbar} v_F\, r_S\, q \left[k_B T \ln 2 - \frac{\Delta^2}{4 k_B T} \left(1 + \ln\left(\frac{\Delta}{2 k_B T} \right) \right) \right] . \tag{26}$$

C. Plasmon Doping at a low temperature for extrinsic graphene

Let us consider the case of a finite doping $\mu > 0$ and low temperature $T \to 0$. We must calculate: the polarization function using

$$\Pi_T^{(0)}(q,\omega;\Delta) = \int_0^{\infty} d\,\mu' \frac{\Pi^0(q,\omega;\Delta)}{4 k_B T \left(\cosh\left[\frac{\mu-\mu'}{2 k_B T} \right] \right)^2} = \int_0^{\Delta} d\,\mu' \ \frac{P_0(q,\omega;\Delta)}{4 k_B T \left(\cosh\left[\frac{\mu-\mu'}{2 k_B T} \right] \right)^2} + \int_{\mu'=\Delta}^{\infty} d\,\mu' \frac{\Pi_{\mu'}^{(0)}(q,\omega,\Delta)}{4 k_B T \left(\cosh\left[\frac{\mu-\mu'}{2 k_B T} \right] \right)^2} .$$

The first term is trivial and given by

$$\int_0^{\mu'=\Delta} \frac{P_0(q,\omega;\Delta)}{4 k_B T \left(\cosh\left[\frac{\mu-\mu'}{2 k_B T} \right] \right)^2} = P_0(q,\omega;\Delta) \frac{1}{2} \left\{ \tanh\left(\frac{\Delta-\mu}{2 k_B T} \right) + \tanh\left(\frac{\mu}{2 k_B T} \right) \right\} . \tag{27}$$

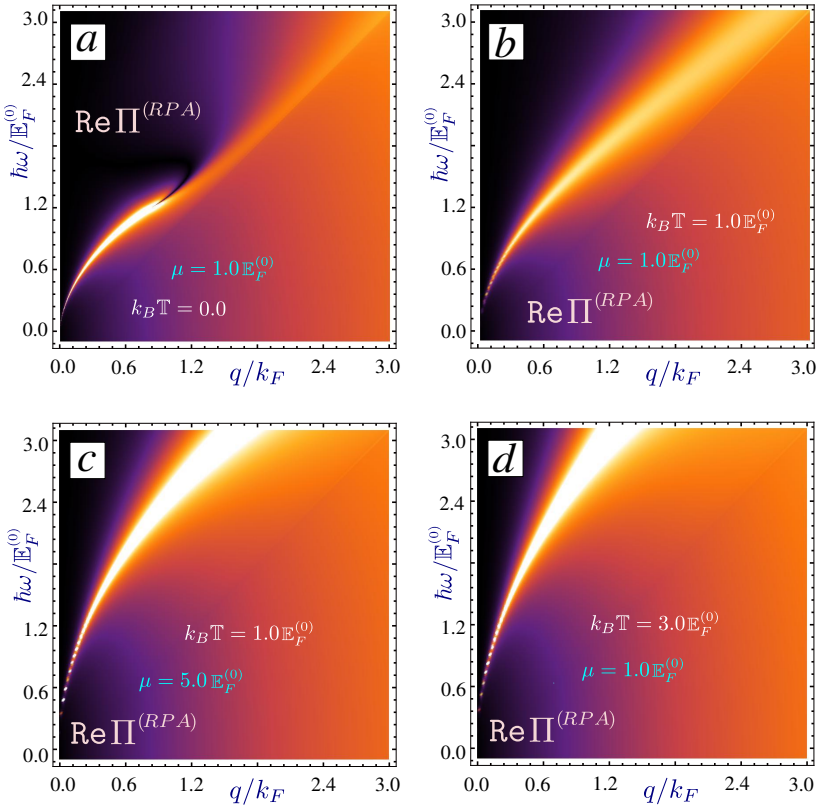

FIG. 2: (Color online) Finite-temperature plasmon excitations in graphene for various chosen values of doping and temperature (density plot of RPA polarization function whose peaks correspond to the plasmon mode frequencies). Panel (a) shows the zero-temperature limit of a graphene plasmon with finite doping $\mu = 1.0\mathbb{E}_F^{(0)}$. Plot ($b$) corresponds to $k_b\mathbb{T} = 1.0\mathbb{E}_F^{(9)}$ and $\mu = 1.0\mathbb{E}_F^{(0)}$. Panels ($c$) and ($d$) show plots of the plasmon dispersion relation for either high temperature or doping value ($k_b\mathbb{T} = 1.0\mathbb{E}_F^{(0)}$ and $\mu = 5.0\mathbb{E}_F^{(0)}$ for (c) and $k_b\mathbb{T} = 3.0\mathbb{E}_F^{(0)}$ and $\mu = 1.0\mathbb{E}_F^{(0)}$ for (d).

In the limit $T \to 0$, it follows that $\tanh(\alpha/T) \to \mathrm{sign}(\alpha)$, so when Eq. (27) gives 2 when $\Delta > \mu$ and 0 when $\Delta < \mu$. So that the integral is $\theta(\Delta - \mu)$. The second term is an integral representation of a Dirac delta-function for $T = 0$ K so that $\delta(x) = \lim_{\epsilon\to 0} \frac{1}{2\epsilon}\cosh^{-2}(x/\epsilon)$ and we have finally

$$\Pi^0(q,\omega;\Delta) = P_0(q,\omega;\Delta) + \theta(\mu - \Delta)\Pi^0_\mu(q,\omega;\Delta) \tag{28}$$

as we had for $T = 0$.

D. Damping rates for gapped graphene

The imaginary part of the zero-temperature polarization function is from Eq. (28) given by

$$Im\ \Pi^0(q,\omega) = \frac{gq^2}{8\hbar\omega}\left\{1 - \frac{1}{2}X_0^2\right\}\theta\left(2\mu - \hbar\omega\right)\,, \tag{29}$$

where

$$X_0 = \sqrt{1 + \frac{4\Delta^2}{\hbar^2\left(v_F^2q^2 - \omega^2\right)^2}} \backsimeq \left(1 - \frac{2\Delta^2}{\hbar^2\omega^2}\right) \tag{30}$$

which gives

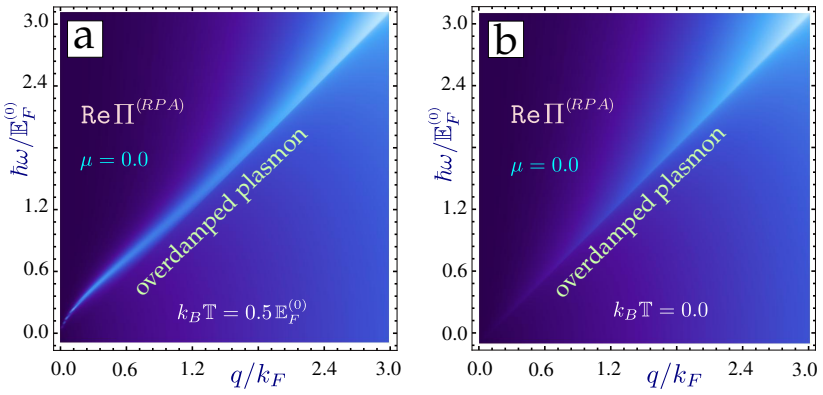

FIG. 3: (Color online) Overdamped (suppressed) plasmon frequencies for graphene at low doping concentration and $T \to 0$. Panel (a) gives the dispersion relation at low temperature $k_b\mathbb{T} = 1.0\mathbb{E}_F^{(0)}$, while panel (b) corresponds to $\mathbb{T} = 0$. Both panels are plotted for intrinsic monolayer graphene.

$$\mathrm{Im}\ \Pi(q,\omega) = \frac{gq^2}{16\hbar\omega}\left\{1 + \frac{4\Delta^2}{\hbar^2\omega^2}\right\}\theta\left(2\mu - \hbar\omega\right) . \tag{31}$$

The finite-temperature polarizability is obtained as follows

$$\mathrm{Im}\ \ \Pi_T^{(0)}(q,\omega) = -i\frac{gq^2}{16\hbar\omega}\left\{1 + \frac{4\Delta^2}{\hbar^2\omega^2}\right\}\int_0^\infty \frac{d\,\mu'}{4k_BT}\frac{\theta(\hbar\omega - 2\mu')}{\cosh^2\left[\frac{\mu-\mu'}{2k_BT}\right]} \tag{32}$$

which has imaginary part

$$\mathrm{Im}\ \ \Pi_T^{(0)}(q,\omega) = i\frac{gq^2}{16\hbar\omega}\left\{1 + \frac{4\Delta^2}{\hbar^2\omega^2}\right\}\frac{1}{2}\tanh\frac{\hbar\omega}{4k_BT} \backsimeq \frac{g}{64}\frac{q^2}{k_BT}\left\{1 + \frac{4\Delta^2}{\hbar^2\omega^2}\right\} . \tag{33}$$

Another correction to the imaginary part of the frequency

$$\mathrm{Im}\ \ P_0(q,\omega;\Delta) = -\frac{1}{4\hbar}\frac{q^2}{\sqrt{\omega^2 - v_F^2q^2}} \tag{34}$$

This shows that when $T = 0$ K, the first-order correction associated with the energy gap is linear, real and negative. At finite temperature, our calculation shows that

$$\mathrm{Im}\ \ I_1 = \frac{1}{2}P_0(q,\omega;\Delta)\tanh\left[\frac{\Delta}{2k_BT}\right] \backsimeq -\frac{i}{4\hbar}\frac{q^2}{\sqrt{\omega^2 - v_F^2q^2}}\frac{\Delta}{2k_BT} \backsimeq -\frac{1}{8\hbar}\frac{\Delta}{k_BT}\frac{q^2}{\omega} . \tag{35}$$

Additionally, making use of similar procedures when we dealt with zero gap, we obtain

$$-\frac{2\gamma}{\omega^3}\frac{q^2}{\pi\hbar^2}k_BT\left\{2\ln 2 - \frac{\Delta^2}{4k^2T^2}\left[C + \ln\left(\frac{\Delta}{2k_BT}\right)\right]\right\} + \frac{1}{16}\frac{q^2}{k_BT}\left\{1 + \frac{4\Delta^2}{\hbar^2\omega^2}\right\} - \frac{1}{8\hbar}\frac{\Delta}{k_BT}\frac{q^2}{\omega} = 0 \tag{36}$$

from which we deduce the damping rate

$$\gamma = \frac{\omega^3}{32}\frac{\pi\hbar^2}{k^2T^2}\left\{1 - \frac{2\Delta}{\hbar\omega} - \frac{2\Delta^2}{\hbar^2\omega^2}\right\} \Big/ \left\{2\ln 2 - \frac{\Delta^2}{4k^2T^2}\left[C + \ln\left(\frac{\Delta}{2k_BT}\right)\right]\right\} \tag{37}$$

which may be rewritten as

$$\gamma = \frac{\pi}{8}\frac{\hbar^{1/2}}{\sqrt{k_BT}}(\ln 2)^{1/2}\left(r_sv_Fq\right)^{3/2} - \frac{1}{8}\frac{r_sv_Fq}{k_BT}\Delta - \left\{\frac{2\sqrt{k_BT}\left(qr_sv_F\right)^{1/2}}{\hbar^{1/2}\sqrt{\ln 2}} - \frac{\left(qv_Fr_s\right)^{3/2}}{\hbar^{3/2}\sqrt{k_BT}\sqrt{\ln 2}}\ln\left[\frac{\Delta}{2k_BT}\right]\right\}\Delta^2 . \tag{38}$$

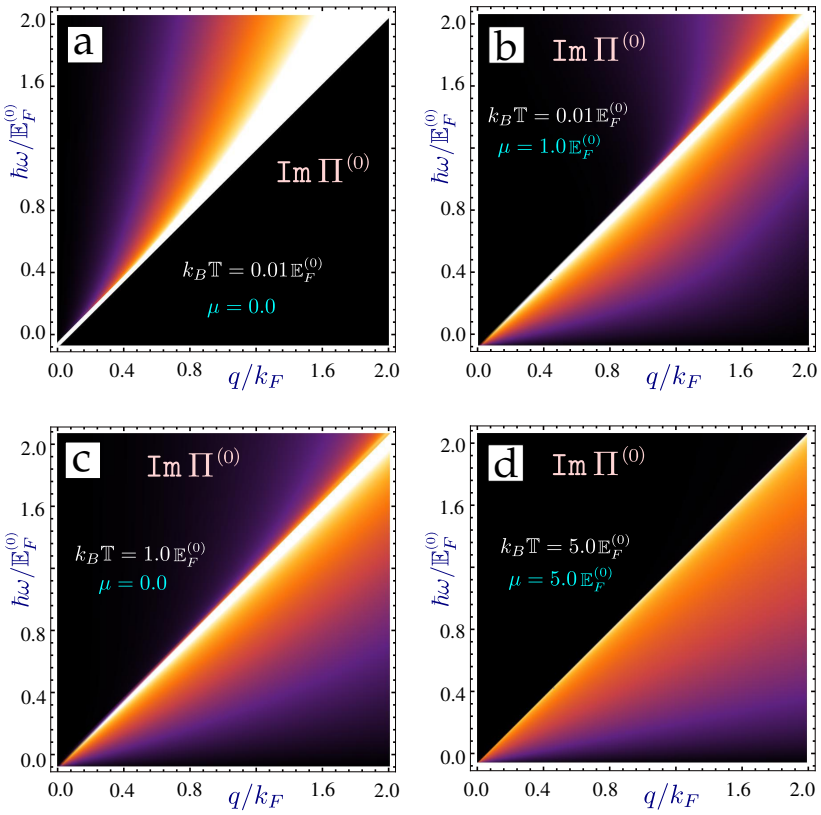

FIG. 4: (Color online) Density plot of the imaginary part of the polarization function at various chosen temperatures and doping concentrations in graphene. Panel (a) shows a plot corresponding to low temperature $k_B\mathbb{T} = 0.01\mathbb{E}_F^{(0)}$ and zero doping (in which plasmons do not exist due to the absence of free carriers). Plot (b) demonstrates the low-temperature limit for finite $\mu = 1.0\mathbb{E}_F^{(0)}$. Panel ($c$) corresponds to finite temperature and zero doping, whereas panel (d) shows the finite-temperature particle-hole modes for highly doped graphene $\mu = 5.0\mathbb{E}_F^{(0)}$.

III. GAPLESS MONOLAYER GRAPHENE INTERACTING WITH A THICK CONDUCTING SUBSTRATE

According to recent work[30,33], the plasma dispersion relations when a 2D layer is Coulomb-coupled to a thick conducting substrate are determined by solving the following equation:

$$1 - v(q)\Pi_T^{(0)}(q,\omega)\left\{1 + \mathrm{e}^{-2aq}\frac{\omega_p^2}{2\omega^2 - \omega_p^2}\right\} = 0\ , \tag{39}$$

where a is the layer-surface separation, ω_p is the bulk plasmon frequency and the Fourier transform of the Coulomb potential energy

$$v(q) = \frac{2\pi e^2}{\varepsilon_s q} = \frac{2\pi}{q}\hbar r_s v_F \tag{40}$$

is expressed in terms of r_s is a dimensionless parameter.

The finite-temperature polarization function is

$$\Pi_T^{(0)}(q,\omega) = \frac{2\ln 2}{\pi}\frac{q^2}{\hbar^2\omega^2}k_BT + \frac{i}{16}\frac{q^2}{k_BT} \tag{41}$$

Here, we consider a well-defined plasmon with $\gamma \ll \omega$, which is excited with a certain wave vector at a chosen temperature. Accordingly, we neglect the contributions to the real part of the polarization function arising from the imaginary part of the frequency. So, making use of

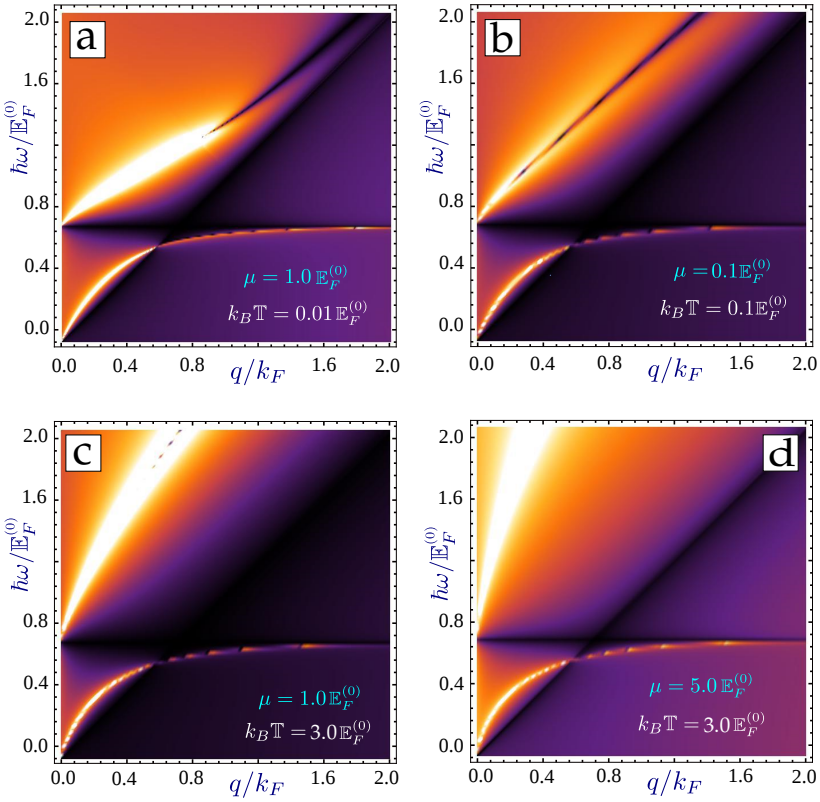

FIG. 5: (Color online) Plasmon dispersion relations for monolayer graphene, which is Coulomb-coupled with a semi-infinite conductor for different chosen values of graphene doping and temperature. Panel (a) shows the low-temperature limit when the doping is finite corresponding to $\mu = 1.0\mathbb{E}_F^{(0)}$. Plot ($b$) and shows the case for $k_b\mathbb{T} = 0.1\mathbb{E}_F^{(0)}$ for a slightly doped graphene $\mu = 0.1\mathbb{E}_F^{(0)}$. Both panels ($c$) and ($d$) correspond to a moderately high temperature $k_B\mathbb{T} = 3.0\mathbb{E}_F^{(0)}$ and different chemical potentials ($\mu = 1.0\mathbb{E}_F^{(0)}$ for (c) and $\mu = 5.0\mathbb{E}_F^{(0)}$ for (d)).

$$\mathrm{Re}\ \ \Pi_T^{(0)}(q,\omega) = \frac{2\ln 2}{\pi}\frac{q^2}{\hbar^2\omega^2}k_BT\,, \tag{42}$$

in Eq. (39), we obtain

$$1 - \frac{2\pi}{q}\hbar r_s v_F \frac{2\ln 2}{\pi}\frac{q^2}{\omega^2}k_BT\left\{1 + \mathrm{e}^{-2aq}\frac{\omega_p^2}{2\omega^2-\omega_p^2}\right\} = 0\,. \tag{43}$$

We rewrite this equation as

$$\begin{aligned} 1 - \lambda\frac{q}{(\omega/\omega_p)^2}\left\{1 + \mathrm{e}^{-2aq}\frac{\omega_p^2}{2\omega^2-\omega_p^2}\right\} &= 0 \\ \lambda = 4\ln 2\left(\frac{r_s v_F}{\hbar\omega_p^2}\right)\ k_BT\ . \end{aligned} \tag{44}$$

We now consider *two* different limiting cases. The first corresponds to when the surface-layer separation is small so that $aq \ll 1$. For this, we have the results in the linear approximation

$$\begin{aligned} \Omega_1 &= \sqrt{8\ln 2\frac{r_s v_F}{\hbar}}\sqrt{a}\sqrt{k_BT}\,q\ . \\ \Omega_2 &= \frac{\omega_p}{\sqrt{2}} + \sqrt{8}\ln 2\,\frac{r_s v_F}{\hbar\,\omega_p}k_BT\,q \end{aligned} \tag{45}$$

Both solutions are linear in q, we also note that the surface plasmon frequency does not depend on a until the second-order terms for the Ω_1. branch. Second-order terms in q are neglected since we are interested in the temperature dependence in the lowest order. Turning now to the set-up when $aq \gg 1$, a straightforward calculation yields

$$\begin{aligned} \frac{\Omega_1}{\omega_p} &= \sqrt{\lambda q} - \frac{1}{2}\frac{\sqrt{\lambda q}}{1-\lambda q}\mathsf{e}^{-2aq}\,, \\ \frac{\Omega_2}{\omega_p} &= \frac{1}{\sqrt{2}} + \frac{1}{\sqrt{2}}\frac{\lambda q}{1-\lambda q}\mathsf{e}^{-2aq}\,. \end{aligned} \tag{46}$$

In the local limit $\lambda q \ll 1$, we obtain

$$\begin{aligned} \Omega_1 &= \sqrt{\frac{2\ln 2}{\hbar}}\left(v_F r_s q\right)^{1/2}\sqrt{k_B T}\left\{1 - \frac{1}{2}\mathsf{e}^{-2aq}\right\}\,, \\ \Omega_2 &= \frac{\omega_p}{\sqrt{2}} + 2\sqrt{2}\ln 2\,\frac{r_s v_F}{\hbar\,\omega_p}k_B T\,q\,\mathsf{e}^{-2aq}\,. \end{aligned} \tag{47}$$

We need to take into account the imaginary part of the $\omega_p^2/(2\omega^2 - \omega_p^2)$ term. We make the replacement $\omega \to \omega + i\gamma$ which leads to the following plasmon dispersion equation

$$1 - \left\{\frac{4\ln 2}{\hbar}r_s v_F k_B T\frac{q}{\omega^2}\left(1 - 2i\frac{\gamma\omega_p^2}{\omega^2}\right) + i\frac{\pi}{8}r_s v_F\hbar\frac{1}{k_B T}q\right\}\left\{1 + \mathsf{e}^{-2aq}\left[\frac{1}{2(\omega/\omega_p)^2 - 1} - 4i\gamma\frac{\omega/\omega_p}{(2(\omega/\omega_p)^2 - 1)^2}\right]\right\} = 0\,, \tag{48}$$

From this, we obtain the imaginary part for the lower "acoustic" branch to be

$$\Gamma_1 = \pi\sqrt{\frac{\ln 2}{2}}\sqrt{\frac{\hbar}{k_B T}}\left(r_s v_F\right)^{3/2} a^{3/2} q^3\,, \tag{49}$$

while the "upper" branch has imaginary part

$$\Gamma_2 = \frac{\pi}{8\sqrt{2}}\hbar v_F r_s\frac{\omega_p}{k_B T}q \tag{50}$$

When the surface-layer separation is large, the imaginary parts may be further approximated as

$$\begin{aligned} \Gamma_1 &= \frac{\pi}{8}\sqrt{\ln 2}\sqrt{\frac{\hbar}{k_B T}}\left(r_s v_F\right)^{3/2} q^{3/2}\left[1 - 8\ln 2\,\frac{r_s v_F}{\hbar\omega_p^2}k_B T\,q\,\mathsf{e}^{-2aq}\right]\,,\,, \\ \Gamma_2 &= \frac{\pi}{16}\hbar\omega_p\frac{r_s v_F}{k_B T}\,q\,\mathsf{e}^{-2aq} \end{aligned} \tag{51}$$

where λ has been defined in Eq. (44). We now investigate how some of these results are affected when a finite energy gap exists between the valence and conduction bands.

IV. PLASMONS IN GAPPED GRAPHENE, COULOMB-COUPLED TO A SEMI-INFINITE CONDUCTOR

The real part of the polarization function may be expressed as

$$\mathrm{Re}\;\Pi_T^{(0)} = \frac{2}{\pi\hbar^2}\frac{q^2}{\omega^2}\left\{k_B T\ln 2 - \frac{\Delta^2}{8k_B T}\left[C - \ln\left(\frac{\Delta}{2k_B T}\right)\right]\right\}\,. \tag{52}$$

Here $C = 1 - c_i \backsimeq 1 + 0.10 \backsimeq 1.10$. Furthermore, the analytic form of Eq. (44) is still valid. However, λ must be replaced by λ_Δ defined as

$$\lambda_\Delta = 4\,\frac{r_s v_F}{\hbar\omega_p^2}\left\{k_B T\ln 2 - \frac{\Delta^2}{8k_B T}\left[C - \ln\left(\frac{\Delta}{2k_B T}\right)\right]\right\}. \tag{53}$$

When $aq \ll 1$, the solutions are given approximately by

$$\begin{aligned}\Omega_1 &= \sqrt{8}\sqrt{a}\sqrt{\frac{r_s v_F}{\hbar}}\left\{k_B T\ln 2 - \frac{\Delta^2}{8k_B T}\left[C - \ln\left(\frac{\Delta}{2k_B T}\right)\right]\right\}^{1/2} q \\ \Omega_2 &= \frac{\omega_p}{\sqrt{2}} + \sqrt{8}\,\frac{r_s v_F}{\hbar\omega_p}\left\{k_B T\ln 2 - \frac{\Delta^2}{8k_B T}\left[C - \ln\left(\frac{\Delta}{2k_B T}\right)\right]\right\} q\,.\end{aligned} \tag{54}$$

on the other hand, when $aq \gg 1$, the solutions are given simpler are given by

$$\begin{aligned}\Omega_1 &= \sqrt{\lambda_\Delta q}\left(1 - 4\mathsf{e}^{-2aq}\right) = 2\sqrt{\frac{r_s v_F}{\hbar}}\left\{k_B T\ln 2 - \frac{\Delta^2}{8k_B T}\left[C - \ln\left(\frac{\Delta}{2k_B T}\right)\right]\right\}^{1/2}\left(1 - 4\mathsf{e}^{-2aq}\right)\sqrt{q} \\ \Omega_2 &= \frac{\omega_p}{\sqrt{2}} + \sqrt{8}\omega_p\lambda_\Delta q\mathsf{e}^{-2aq} = \frac{\omega_p}{\sqrt{2}} + 8\sqrt{2}\,\frac{r_s v_F}{\hbar\omega_p}\left\{k_B T\ln 2 - \frac{\Delta^2}{8k_B T}\left[C - \ln\left(\frac{\Delta}{2k_B T}\right)\right]\right\} q\mathsf{e}^{-2aq}\,.\end{aligned} \tag{55}$$

We now turn to presenting and discussing our numerical results in the next section.

V. NUMERICAL RESULTS AND DISCUSSION

The plasmon dispersion relations and damping rates for gapped graphene in the long-wavelength limit are presented in Fig. 1. The plasmon frequency is increased at higher temperature, approximately having the behavior of $\backsimeq \sqrt{T}$ dependence as for gapless graphene. Clearly, the damping rates decrease with increasing energy gap for all temperatures. This means that the plasmon modes become less damped in the presence of a finite energy gap.

We are definitely interested in calculating the polarization function and plasmon energies numerically beyond the long wavelength limit. First, we obtain the imaginary part of the polarization function in Fig. 4, looking for the regions within $\{q-\omega\}$-plane where the relatively undamped plasmon modes exist $\left(\mathrm{I}m\ \Pi^{(0)}(q,\omega)\to 0\right)$. As we know for the long wavelength limit, the imaginary part of the polarization function within the region of graphene plasmon excitations decreases at high temperature as $\backsimeq 1/T$,[10] so it is relatively small at high temperatures although it not be negligible. Panel (b) of Fig. 4 demonstrates the behavior when$\mu = \mathbb{E}_F^{(0)}$ at very low temperature, which approximately corresponds to the standard particle-hole modes of zero-temperature graphene.[7] We see that at finite doping and high temperature, the region of particle-hole modes (finite $\mathrm{I}m\ \Pi^{(0)}(q,\omega)$) above the diagonal $\omega = v_F q$ is suppressed, as shown in panel (d).

Figure 2 presents the RPA polarizability for various doping concentrations and temperatures. At zero temperature and when the doping is finite, we reproduce the well-known plasmon dispersion relation in graphene, as it was reported in Ref. [7]. As the temperature is increased, the plasmon frequency is also increased for all values of the wave vector, growing with temperature like $\sqrt{T}$ in the long wavelength limit as it was showed analytically in Ref.[10]). Various examples of damped plasmon excitations are shown in Fig. 3. As it was mentioned above as well as in Ref.[10], the plasmon mode has low intensity in the limit of vanishing temperature and zero doping.

The temperature-dependent plasmon dispersion relation for a graphene monolayer interacting with a semi-infinite conductor is shown in Fig. 5. There are clearly two plasmon branches, originating from the graphene layer (acoustic branch, starting at the origin), and the "sruface plasmon", which is depolarization shifted from its long wavelength value of at $1/\sqrt{2}\omega_p$. Both branches have positive group velocity for $(q\to 0)$, i.e. are linear in the long-wave limit, similarly to its variation at zero temperature. Another interesting detail, which deserves mentioning is that the higher plasmon branch, attributed to the surface behaves similarly to the plasmons in graphene (see Fig. 2), while the lower acoustic branch remains nearly unchanged for all the chosen temperature and doping values.

The plasmon frequencies and the damping rates for grpahene, Coulomb-coupled with a thick conductor with free carriers in the long wavelength limit are presented in Fig. 6. Both plasmon dispersions are linear and increase with temperature as $\backsimeq \sqrt{T}$ and $\backsimeq T$, respectively. We also note that the damping rate Γ_2, which corresponds to the upper plasmon, depends linearly on the wave vector q. This is a new result, which was not encountered in graphene, either with a finite or zero energy gap.

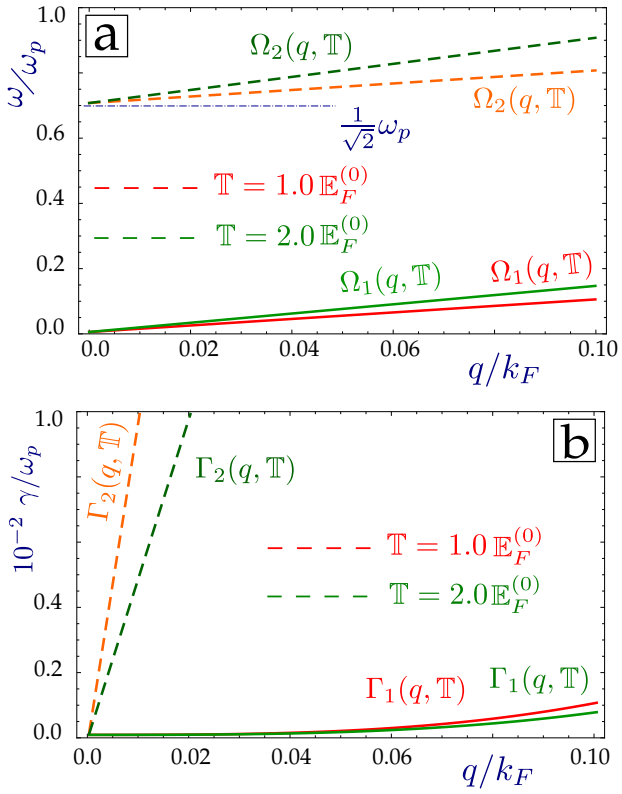

FIG. 6: (Color online) (a) Plasmon frequencies and (b) the damping rates in the high-temperature limit for monolayer graphene interacting with a semi-infinite conductor in the long wavelength limit. Each plasmon branch (both real and imaginary parts) are presented at two chosen temperatures - $k_B\mathbb{T}=1.0\mathbb{E}_F^{(0)}$ and $k_B\mathbb{T}=2.0\mathbb{E}_F^{(0)}$.

VI. CONCLUDING REMARKS

In summary, we have obtained analytic expressions for the high-temperature plasmon dispersion relations for gapped graphene, as well as for a graphene layer interacting with a semi-infinite conductor. We have found that the plasmon frequency is modified according to $\Delta^2/(4k_BT)\ln(\Delta/(2k_BT))$ in the presence of an energy gap, which is different from the case when $T=0$. The corresponding damping rate is decreased linearly in the presence of a gap, making the plasmon more stable compared to its counterpart for gapless graphene. Our investigation of a graphene monolayer, which is Coulomb-coupled to a semi-infinite metal, revealed a number of novel features for both plasmon frequencies and the damping rates. Specifically, we emphasize the linear $q-$dependence of some of the damping rates, which has not been encountered for graphene (either gapped or ungapped).

Acknowledgments

This research was supported by contract # FA 9453-13-1-0291 of AFRL.

Appendix A: Finite temperature polarization - integral transformation derivation

In this Appendix, we prove that the finite-temperature polarizability could be expressed as an integral transformation given in Eq. (A1) relating the polarization function $\Pi_T^{(0)}(q,\omega)$ at zero temperature, as it was reported in Ref.[10].

We need to prove the general validity of the following expression:

$$\Pi_T^{(0)}(q,\omega) = \int\limits_0^\infty d\mu' \ \frac{\Pi^0(q,\omega)}{4k_BT\left(\cosh\left[\frac{\mu-\mu'}{2k_BT}\right]\right)^2} \tag{A1}$$

with the zero-temperature polarization function is as follows:

$$\Pi^0(q,\omega) = \frac{g}{4\pi^2}\int d^2\mathbf{k} \ \ f^{ss'}(\mathbf{q},\mathbf{k})\frac{n_F\left[\varepsilon^s(k)\right] - n_F\left[\varepsilon^{s'}(|\mathbf{k}+\mathbf{q}|)\right]}{\varepsilon^s(k) - \varepsilon^{s'}(|\mathbf{k}+\mathbf{q}|) + \hbar(\omega+i\gamma)} \tag{A2}$$

in terms of the spin and valley degeneracy factor $g = 4$ and the form factor $f^{ss'}(\mathbf{q},\mathbf{k})$. The only temperature-dependent terms in Eq. (A2) are the Fermi-Dirac distribution functions $n_F(\varepsilon) = (1+\mathtt{exp}[(\varepsilon-\mu)/(k_BT)])^{-1} = (1+\mathtt{exp}[\beta(\varepsilon-\mu)])^{-1}$ with $\beta = 1/(k_BT)$. This means that we must prove a similar integral transformation for the distribution functions.

The Fermi-Dirac distribution functions could be presented as

$$n_F(\xi) = \frac{1}{2}\left(1 - \tanh\frac{\beta\xi}{2}\right), \tag{A3}$$

where $\xi = \varepsilon - \mu$. Indeed,

$$1 - \frac{2}{1+\mathtt{e}^{\beta\xi}} = \frac{\mathtt{e}^{\beta\xi}-1}{\mathtt{e}^{\beta\xi}+1} = \frac{\mathtt{e}^{\beta\xi/2}-\mathtt{e}^{\beta\xi/2}}{\mathtt{e}^{\beta\xi/2}+\mathtt{e}^{\beta\xi/2}} = \tanh\frac{\beta\xi}{2} \tag{A4}$$

While at zero temperature, the distribution function could be presented as the Heaviside unit step with $n_F(\varepsilon-\mu, T\to 0) = \theta(\mu-\varepsilon)$. Accordingly,

$$\int\limits_0^\infty \frac{\theta(\mu-\varepsilon)d\,\mu'}{4k_BT\cosh^2[(\mu-\mu')/(2k_BT)]} = \int\limits_\varepsilon^\infty \frac{d\,\mu'}{4k_BT}\cosh^{-2}\left[\frac{\mu-\mu'}{2k_BT}\right]. \tag{A5}$$

We substitute $\eta = \frac{\mu-\nu'}{2k_BT}$ so that $d\,\mu' = -2k_BTd\,\eta$. The limits of integration now become $\eta_< = \frac{\mu-\varepsilon}{2k_BT}$ and $\eta_> = -\infty$. Obviously, $\eta_< > \eta_>$. The integral now takes the form

$$\int\limits_{\eta_<}^{-\infty} \frac{-2k_BTd\,\eta}{4k_BT\cosh^2[\eta]} = \frac{1}{2}\int\limits_{-\infty}^{\eta_<}\frac{d\,\eta}{\cosh^2\eta} = \frac{1}{2}\tanh\eta|_\infty^{\eta_<} = \frac{1}{2}\left(\tanh\eta_< + 1\right). \tag{A6}$$

Also we can write

$$\tanh\eta_< = \tanh\left[\frac{\mu-\varepsilon}{2k_BT}\right] = -\tanh\left[\frac{\beta}{2}(\varepsilon-\mu)\right]. \tag{A7}$$

Finally, we obtain

$$n_F(\xi) = \frac{1}{2}\left(1-\tanh\frac{\beta\xi}{2}\right) = \int\limits_0^\infty d\,\mu' \ \frac{\theta(\mu-\varepsilon)}{4k_BT\cosh^2[(\mu-\mu')/(2k_BT)]} \tag{A8}$$

Alternatively, we have

$$n_F(\varepsilon,\mu;T) = \int\limits_0^\infty \frac{n_F(\varepsilon,\mu';T=0)\ d\,\mu'}{4k_BT\cosh^2[(\mu-\mu')/(2k_BT)]}. \tag{A9}$$

Appendix B: Derivation of the long wavelength limit of the Polarization Function[7–9] and the Finite-temperature Plasmon Modes[10]

First we need to derive the long-wave limit of the polarization with $q \to 0$ with fixed frequency $\omega \gg v_F q$. We consider two separate cases with different imaginary part of the polarization: 1) $\omega > 2\mu$ and 2) $\omega < 2\mu$.

$$\Pi^0(q,\omega) = \frac{gq^2}{8\pi\hbar\omega}\left\{\frac{2\mu}{\hbar\omega} + \frac{1}{2}\ln\left|\frac{2\mu-\hbar\omega}{2\mu-\hbar\omega}\right| - \frac{\mathrm{i}\pi}{2}\theta(\hbar\omega-2\mu)\right\} \tag{B1}$$

If we consider the region with $\hbar\omega \ll \mu$, we can simplify as follows:

$$\ln\left|\frac{2\mu-\hbar\omega}{2\mu-\hbar\omega}\right| \backsimeq -\frac{\hbar\omega}{2\mu} \tag{B2}$$

Finally, for the region $1A$ (where the zero-temperature plasmons exist), we have

$$\begin{aligned} &\mathrm{R}e\ \ \Pi^0(q,\omega) = \frac{gq^2}{8\pi\hbar\omega}\frac{2\mu}{\hbar\omega} = \frac{\mu}{\pi\hbar^2}\frac{q^2}{\omega^2} \\ &\mathrm{I}m\ \ \Pi^0(q,\omega) = 0, \qquad\qquad (\hbar\omega < 2\mu) \end{aligned} \tag{B3}$$

1. Derivation of Eq.(B1)

The general exression for the non-interacting polarization functions is:

$$\Pi^0(q,\omega) = P_0(q,\omega) + \delta P(q,\omega) \tag{B4}$$

with the term $P_0(q,\omega)$, corresponding to the inter-band transitions, which is urely imaginary for $\omega > v_F q$ and the μ-dependent $\delta P(q,\omega)$, which appears due to the inrta-band transitions inside the conduction band (for $\mu > 0$). The terms could be introduced in the following form

$$\begin{aligned} P_0(q,\omega) &= -\frac{i\pi}{\hbar^2 v_F^2} F_1(q,\omega) \\ \delta P(q,\omega) &= -\frac{g\mu}{2\pi\hbar^2 v_F^2} + \frac{1}{\hbar^2 v_F^2} F_1(q,\omega)\left\{F_2\left(\frac{\hbar\omega+2\mu}{\hbar v_F q}\right) - F_2\left(\frac{2\mu-\hbar\omega}{\hbar v_F q}\right) - i\pi\right\} \end{aligned} \tag{B5}$$

with

$$\begin{aligned} F_1(q,\omega) &= \frac{g}{16\pi}\frac{\hbar v_F^2 q^2}{\sqrt{\omega^2 - v_F^2 q^2}} \\ F_2(\mathcal{X}) &= \mathcal{X}\sqrt{\mathcal{X}^2-1} - \ln(\mathcal{X}+\sqrt{\mathcal{X}^2-1}) \qquad (\mathcal{X} > 1) \end{aligned} \tag{B6}$$

Eq.(B5) is satisfied in the `Region 1A`, given as $\omega < 2\mu - v_F q$ and $\omega > v_F q$. Now let us consider each term for $q \to 0$ and $v_F q \ll \omega$. We start with the following approximation

$$\frac{1}{\sqrt{\omega^2 - v_F^2 q^2}} = \frac{1}{\omega}\left(1 - \left(\frac{v_F q}{\omega}\right)^2\right)^{-1/2} \backsimeq \frac{1}{\omega} + \frac{(v_F q)^2}{2\omega^3} + \frac{3}{8}\frac{v_F^4 q^4}{\omega^5} \tag{B7}$$

Consequently, the inter-band polarization function has the form

$$P_0(q,\omega) = -\frac{i\pi}{\hbar}\frac{q^2}{\omega} - \frac{i\pi}{\hbar}\frac{v_F^2 q^4}{2\omega^3} + \dots, \tag{B8}$$

i.e. is purely imaginary.

Now we consider the intra-band part $\delta P(q,\omega)$. First, we analyze how each term of it behaves for $q \to 0$. Thus

$$\mathcal{X} = \frac{2\mu \pm \hbar\omega}{\hbar v_F q} \gg 1 \tag{B9}$$

and

$$F_2(\mathcal{X}) = \mathcal{X}\sqrt{\mathcal{X}^2-1} - \ln[\mathcal{X}+\sqrt{\mathcal{X}^2-1}], \qquad (\mathcal{X}\gg 1) \tag{B10}$$
$$\mathcal{X}\sqrt{\mathcal{X}^2-1} = \mathcal{X}^2(1-1/\mathcal{X}^2)^{1/2} \backsimeq \mathcal{X}^2 - \frac{1}{2}$$
$$\mathcal{X} - \sqrt{\mathcal{X}^2-1} = \mathcal{X}^2 - \mathcal{X}\left(1-\frac{1}{2\mathcal{X}^2}\right) \backsimeq \mathcal{X}^2 - \mathcal{X}$$

Let us summarize the results:

$$F_2\left(\frac{\hbar\omega+2\mu}{\hbar v_F q}\right) - F_2\left(\frac{\hbar\omega-2\mu}{\hbar v_F q}\right) \backsimeq \left(\frac{\hbar\omega+2\mu}{\hbar v_F q}\right)^2 - \frac{1}{2} - \left(\frac{\hbar\omega-2\mu}{\hbar v_F q}\right)^2 + \frac{1}{2} - \ln\left[\left(\frac{\hbar\omega+2\mu}{\hbar v_F q}\right)^2\right] + \ln\left[\left(\frac{\hbar\omega-2\mu}{\hbar v_F q}\right)^2\right] =$$
$$= \frac{2\times 4\hbar\omega\mu}{(\hbar v_F q)^2} + 2\ln\left[\frac{2\mu-\hbar\omega}{2\mu+\hbar\omega}\right] \tag{B11}$$

and also

$$\frac{1}{\hbar^2 v^2}F_1(q,\omega) \backsimeq \frac{g}{16\pi\hbar}\frac{q^2}{\omega} + \frac{g}{32\pi\hbar}\frac{v_F^2 q^4}{\omega^2} \tag{B12}$$

As a result

$$\frac{1}{\hbar^2 v^2}F_1(q,\omega)\left[F_2\left(\frac{\hbar\omega+2\mu}{\hbar v_F q}\right) - F_2\left(\frac{\hbar\omega-2\mu}{\hbar v_F q}\right)\right] = \frac{\mu g}{2\pi\hbar^2 v_F^2} + \frac{gq^2}{4\hbar^2}\frac{\mu}{\pi\omega^2} \tag{B13}$$

Finally, we can write

$$\mathrm{R}e\ \delta P(q,\omega) = -\frac{g\mu}{2\pi\hbar^2 v_F^2} + \frac{\mu g}{2\pi\hbar^2 v_F^2} + \frac{gq^2}{8\pi\hbar\omega}\left(\frac{2\mu}{\hbar\omega}\right) + \frac{gq^2}{16\pi\hbar\omega}\ln\left[\frac{2\mu-\hbar\omega}{2\mu+\hbar\omega}\right] \tag{B14}$$

As far as the imaginary part is concerned, it is equal to zero everywhere in `Region 1A`:

$$\mathrm{I}m\ \delta P(q,\omega) = i\pi\frac{F_1(q,\omega)}{\hbar^2 v_F^2} \tag{B15}$$

According to Eq.(B5)

$$P_0(q,\omega) = -\frac{i\pi}{\hbar^2 v_F^2}F_1(q,\omega) \tag{B16}$$

so that

$$\Pi^0(q,\omega) = P^0(q,\omega) + \delta P(q,\omega) = 0 \tag{B17}$$

So Eq.(B1) is confirmed.

2. Finite-temperature plasmons

The finite temperature non-interaction polarization function is expressed as follows:

$$\Pi_T^{(0)}(q,\omega) = \int_0^\infty \frac{\Pi^0(q,\omega)}{4k_B T\left(\cosh\left[\frac{\mu-\mu'}{2k_B T}\right]\right)^2} \tag{B18}$$

In the long-wave limit approximation, the zero-temperature polarizability is as follows:

$$\Pi^0(q,\omega) = \frac{gq^2}{4\pi}\frac{\mu}{(\hbar\omega)^2} - i\frac{gq^2}{16\hbar\omega}\theta(\hbar\omega-2\mu) \tag{B19}$$

Let us first consider the real part:

$$\mathrm{Re}\ \Pi_T^{(0)} = \int\limits_0^\infty \frac{gq^2}{4\pi}\frac{\mu'}{(\hbar\omega)^2}\frac{1}{4k_BT}\frac{d\,\mu'}{\cosh^2\left[(\mu-\mu')/(2k_BT)\right]} = \frac{gq^2}{4\pi\hbar^2\omega^2}\frac{1}{4k_BT}\int\limits_0^\infty \frac{\mu'\ d\,\mu'}{\cosh^2\left[\frac{\mu-\mu'}{2k_BT}\right]} \tag{B20}$$

This integral could be easily evaluated:

$$\int\limits_0^\infty \frac{\mu'\ d\,\mu'}{\cosh^2\left[\frac{\mu-\mu'}{2k_BT}\right]} = 4k^2T^2\ln\left[1+\mathsf{e}^{\beta\mu}\right] \tag{B21}$$

We consider *intrinsic* graphene with $\mu = 0$ so that $\ln\left[1+\mathsf{e}^{\beta\mu}\right] = \ln 2$.

Thus

$$\mathrm{Re}\ \Pi_T^{(0)}(q,\omega) = \frac{g\ln 2}{2\pi}\frac{q^2}{\hbar^2\omega^2}k_BT \tag{B22}$$

The imaginary part is as following:

$$\mathrm{Im}\ \Pi_T^{(0)}(q,\omega) = -i\frac{gq^2}{16\hbar\omega}\int\limits_0^\infty \frac{d\,\mu'}{4k_BT}\frac{\theta(\hbar\omega-2\mu')}{\cosh^2\left[\frac{\mu-\mu'}{2k_BT}\right]} \tag{B23}$$

Finally

$$\mathrm{Im}\ \Pi_T^{(0)}(q,\omega) = i\frac{gq^2}{16\hbar\omega}\frac{1}{2}\tanh\frac{\hbar\omega}{4k_BT} \backsimeq i\frac{g}{128}\frac{q^2}{k_BT} \tag{B24}$$

3. plasmons

Now we rewrite the finite-temperature polarization function:

$$\Pi_T^{(0)}(q,\omega) = \frac{2\ln 2}{\pi}\frac{q^2}{\hbar^2\omega^2}k_BT + \frac{i}{16}\frac{q^2}{k_BT} \tag{B25}$$

The dielectric function $\epsilon(q,\omega)$ is

$$\epsilon(q,\omega) = 1 - V(q)\Pi_T^{(0)}(q,\omega) \tag{B26}$$

where $V(q) = 2\pi e^2/(\epsilon_s q)$.

We introduce real and imaginary parts of the frequency $\omega \to \omega + i\gamma$ and $r_s = e^2/(\epsilon_s\hbar v_F)$, we find the real part:

$$1 - \frac{2\pi e^2}{\epsilon_s q}\frac{2\ln 2}{\pi}\frac{q^2}{\hbar^2\omega^2}k_BT = 0 \tag{B27}$$

we obtain:

$$\omega^2 = \frac{4\ln 2}{\hbar}v_F\, r_S\, q\, k_BT \tag{B28}$$

Appendix C: Imaginary part of the frequency

For $\Delta = 0$ the polarization function is

$$\Pi_T^{(0)}(q,\omega) = \frac{2\ln 2}{\pi}\frac{q^2}{\hbar^2\omega^2}k_BT + \frac{i}{16}\frac{q^2}{k_BT} \tag{C1}$$

The plasmons are defined by the following equation

$$\epsilon(q,\omega) = 1 - \frac{2\pi e^2}{\epsilon_s q}\Pi_T^{(0)}(q,\omega) = 1 - \frac{2\pi}{q} r_s \hbar v_F \Pi_T^{(0)}(q,\omega) = 0 \tag{C2}$$

Let us introduced the complex frequency:

$$\omega \Longrightarrow \omega + i\gamma \tag{C3}$$

$$\frac{1}{\omega^2} \Longrightarrow \frac{1}{(\omega + i\gamma)^2} \backsimeq \frac{1 - 2i\gamma/\omega}{\omega^2} = \frac{1}{\omega^2} - 2i\frac{\gamma}{\omega^3} \tag{C4}$$

This results in the following equation

$$1 - \frac{2\pi}{q} r_s \hbar v_F \left\{ \frac{2\ln 2}{\pi\hbar^2} q^2 k_B T \left(\frac{1}{\omega^2} - \frac{2i\gamma}{\omega^3} \right) + \frac{i}{16} \frac{q^2}{k_B T} \right\} = 0 \tag{C5}$$

According to Eq.(B28),

$$1 - \frac{2\pi}{q} r_s \hbar v_F \left\{ \frac{2\ln 2}{\pi\hbar^2} q^2 k_B T \frac{1}{\omega^2} \right\} = 0 \tag{C6}$$

which leads to

$$- \frac{2\ln 2}{\pi\hbar^2} q^2 k_B T \frac{2i\gamma}{\omega^3} + \frac{i}{16} \frac{q^2}{k_B T} = 0 \tag{C7}$$

and

$$\gamma = \frac{\pi\hbar^2}{\ln 2} \frac{\omega^3}{64 k^2 T^2} \tag{C8}$$

$$\omega^3 = 8\hbar^{-3/2} (\ln 2)^{3/2} v_F^{3/2} r_S^{3/2} q^{3/2} (k_B T)^{3/2} \tag{C9}$$

$$\gamma = \frac{\pi}{8} \frac{\hbar^{1/2}}{\sqrt{k_B T}} (v_F r_s q)^{3/2} \tag{C10}$$

---

[1] D. S. L. Abergela, V. Apalkov, J. Berashevicha, K. Ziegler, and Tapash Chakraborty, Adv. Phys. **59**, 261 (2010).
[2] G. Gumbs and D. H. Huang: Properties of Interacting Low-Dimensional Systems (Wiley-VCH Verlag GmbH & Co. KGaA, Boschstr, Weinheim, 2011).
[3] R. Roldan, M. O. Goerbig and J.-N. Fuchs, Phys. Rev. B **80**, 085408 (2009).
[4] A. Politano and G. Chiarello, Carbon **71**, 176 (2014).
[5] A. Politano and G. Chiarello, Nanoscale **6**, 10927 (2014).
[6] A. Politano, V. Formoso, and G. Chiarello, J. Phys.: Condens. Matter **25**, 345303 (2013).
[7] B Wunsch, T Stauber, F Sols, and F. Guinea, New J. Phys. **8**, 318 (2006).
[8] P. K. Pyatkovskiy, J. Phys.: Condens. Matter **21**, 025506 (2009).
[9] E. H. Hwang and S. Das Sarma, Phys. Rev. B **75** (20), 205418 (2007).
[10] S. Das Sarma and Q. Li, Phys. Rev. B **87**, 235418 (2013).
[11] P. Nordlander, C. Oubre, E. Prodan, K. Li, and M. I. Stockman, Nano Lett., **4**, 5 (2004).
[12] Gumbs, Godfrey, Antonios Balassis, Andrii Iurov, and Paula Fekete, The Scientific World Journal 2014 (2014).
[13] G. Gumbs, A. Iurov, A. Balassis, and D.H. Huang, J. Phys.: Condens. Matter **26**, 135601 (2014).
[14] Andrii Iurov, Godfrey Gumbs, Bo Gao, and Danhong Huang, Appl.Phys.Lett. **104** , 203103 (2014).
[15] Antonios Balassis and Godfrey Gumbs, Phys. Rev. B **90**, 075431 (2014).
[16] Liubov Zhemchuzhna, Godfrey Gumbs, Andrii Iurov, Danhong Huang, and Bo Gao, Phys. Plasmas **22**, 032116 (2015)
[17] Cheng-Cheng Liu, Wanxiang Feng, and Yugui Yao, Phys. Rev. Lett. **107**, 076802 (2011).
[18] C. J. Tabert and E. J. Nicol, Phys. Rev. B **89**, 195410 (2014).
[19] M. F. Lin and K. W. Shung, Phys. Rev. B **50** , 23, 17744 (1994).

[20] Y. Wang, X. Wang, Q. Wu, X. J. He, T. L. Gui, and Y. J. Tong, Plasmonics **7**, 411-415 (2012).
[21] O. V. Kibis, Phys. Rev. B **81**, 165433 (2010).
[22] M. Busl, G. Platero, and A.-P. Jauho, Phys. Rev. B **85**, 155449 (2012).
[23] G. Giovannetti, P. A. Khomyakov, G. Brocks, V. M. Karpan, J. van den Brink, and P. J. Kelly, Phys. Rev. Lett. **101**, 026803 (2008).
[24] K. L. Grosse, M.-H. Bae, F. Lian, E. Pop, and W. P. King, Nat. Nanotech. **6**, 287 (2011).
[25] N. Reckinger, A. Vlad, S. Melinte, J.F. Colomer, and M. Sarrazin, Appl. Phys. Lett. **102**, 211108 (2013).'
[26] A. V. Zayats, I. I. Smolyaninov, and A. A. Maradudin, Phys. Rep. **408**, 131 (2005).
[27] A. R. Halpern, J. B. Wood, Y. Wang, and R. M. Corn, ACS Nano **8**, 1022 (2014).
[28] W. Srituravanich, N. Fang, C. Sun, Q. Luo, and X. Zhang, Nano Lett. **4**, 1085 (2004).
[29] Godfrey Gumbs, Andrii Iurov and Danhong Huang, arXiv:1410.2851 [cond-mat.mtrl-sci] (2014).
[30] Godfrey Gumbs, Andrii Iurov and N. J. M. Horing, arXiv:1412.7198 [cond-mat.mtrl-sci] (2015).
[31] S. Das Sarma and A. Madhukar, Phys. Rev. B **23**, 805 (1981).
[32] N. J. M. Horing, Phys. Rev. B **80**, 193401 (2009).
[33] N. J. M. Horing, E. Kamen, and H.-L. Cui, Phys. Rev. B **32**, 2184 (1985).